Effect of annealing temperatures on the turn-on voltage of organic Schottky diode based on DPP(BTFu)$_2$

Mahdi Mansour, Mohamed Saidi, Nadia Saidi-Amroun ✉

Material Physics Laboratory, University of Science and Technology Houari Boumediene, Bab Ezzouar, Algiers 16111, Algeria
✉ *E-mail: amnadster@gmail.com*

Published in Micro & Nano Letters; Received on 18th May 2016; Revised on 27th June 2016; Accepted on 20th July 2016

The electrical properties of diketopyrrolopyrrole ethyl-hexylated (DPP(TBFu)$_2$) thin film sandwich structure of the ITO/DPP(TBFu)$_2$/Al configuration for different annealing temperatures ranging from 40 to 130°C is investigated. The current–voltage characteristics showed an excellent rectifying behaviour of the device, and from which the diode parameters were extracted. It is found that all parameters remain constant upon annealing temperatures, with the exception of the turn-on voltage. An increase of the turn-on voltage from an initial value of 1.6–2.08 V is noticed starting from 70 to 100°C, respectively. This fact is attributed to the effect of residual solvent induced defect states that may act as free carriers. Defect states density for the non-annealed and annealed device at 130°C derived from capacitance–voltage measurements is found to correlate well with the turn-on voltage. It is found that annealing the device at 130°C results in a smaller concentration of defect states. In addition, it is also found that the annealing process produces the flat band voltage drop, which has a direct impact on the turn-on voltage.

1. Introduction: Organic semiconductors including small molecules and macromolecular materials are a topic under intense research worldwide with in both the fundamental and industrial point of view. Actually, this class of materials is being considered as an alternative to the inorganic semiconductors that can provide low cost synthesis, and good environmental stability [1]. Specifically, due to their particular properties such as light weight and flexibility, they have emerged as new materials for organic electronic applications [2–4] where they are involved in the active layer and/or operate as carriers transport layers. In general, most of the molecular electronic devices architectures consist on the fabrication of junction devices in which metals and organic semiconductors are stacked on top of each other. Therefore, it is worth noting that these devices should contain at least one metal/semiconductor rectifying contact. Accordingly, investigating organic semiconductor bridging two conductive contacts is a power tool to elucidate the device reliability issues. For example, the current density and the power dissipation of such rectifying contact are strongly influenced by the turn-on voltage and the series resistance of the contact itself [5]. Single layer organic Schottky diodes have already been the subject of great attention. In the literature, most of the devoted works are emphasised on the use of semiconducting polymers such as polyaniline [6], polyacetylene [7], poly(3-methylthiophene) [8], and others [9] as an active component. By contrast, devices based on small molecules have been little investigated. Shah *et al.* [10] have investigated the electrical behaviour of a Schottky diode based on copper phtalocyanine (CuPc) thin film thermally sublimed of the Ag/CuPc/Au structure. Sharma *et al.* [11] have reported capacitance spectroscopy measurements to identify and characterise defect states of thin films based on triple sublimed CuPc grown under high vacuum in an oil free evaporation system making either Al or Au as top and bottom electrodes. Güllü *et al.* [12] have estimated various electronic parameters of a Schottky diode based on Orange G such as the ideality factor, the series resistance, and the barrier height from the current–voltage (I–V) and the capacitance–voltage (C–V) measurements. Recently, various authors have studied Schottky diodes based on pentacene using impedance spectroscopy [13], and I–V for electrical and stability performances [14, 15]. Small molecules are expected to be as a promising alternative to their polymeric analogues for organic electronic technology. Considering small molecules semiconductors which seem to have important interest, some of the advantages that they offer over their polymeric counterparts are the easiest of purification and good reproducibility [16]. Among them, diketopyrrolopyrrole (DPP) derivatives have attracted great attention in organic electronic field few years ago. Devices based on organic pigments to which DPP belongs have reached the promising efficiencies as organic field effect transistor, and organic solar cells. Stability speaking, several factors related to the devices architecture need to be taken into account. Among them, interfaces with the external contact have a crucial role in judging the device reliability. According to that, simple single layer device could be as a good abbreviating tool to elucidate the device performance. Therefore, we have selected the ethyl-hexyl substituted DPP derivative (DPP(TBFu)$_2$) in this work as an active component of a Schottky diode. The goal is to investigate the annealing temperatures effect on the Schottky parameters of DPP(BTFu)$_2$ sandwiched between conductive electrodes (ITO, Al).

2. Experimental part: DPP(TBFu)$_2$ powder has been chemically synthesised according to the method described elsewhere [17]. Solution processed DPP(TBFu)$_2$ was prepared from a DPP (TBFu)$_2$ (2.9 mg) in chloroform (0.25 ml) and was ultrasonically stirred for 30 min at ambient temperature. The organic Schottky diode of structure indium–tin–oxide (ITO)/DPP (DPP(TBFu)$_2$)/aluminium (Al) was then fabricated according to the following procedure: a commercial ITO coated glass substrate of 4 Ω/sq. was cleaned with ultrasonic baths of deionised water and soap, deionised water, acetone, and finally with isopropanol for 5 min during each cycle to remove any residual dust. The DPP(TBFu)$_2$ was then spin coated over clean ITO at 1200 rpm for 15 s. A film thickness of about 90 nm measured by profilometric technique is thus obtained. Before the deposition procedure, the solution processed DPP(TBFu)$_2$ was first filtered by a 0.45 mm nylon filter to exclude the undissolved particles. Then the diode fabrication was completed by thermal evaporation of Al at room temperature under high vacuum ($\sim 4 \times 10^{-6}$ mbar). The active areas are defined from ITO contacts and are about 0.04675 cm^2. Finally, the diode was properly encapsulated using an epoxy resin and glass slide, and then exposed to UV light for 15 min. The

doi: 10.1049/mnl.2016.0318

molecular structure of DPP(TBFu)$_2$, and the corresponding sandwich arrangement of the studied device are shown in Figs. 1*a* and *b*.

Current density–voltage (*J–V*), capacitance–voltage (*C–V*), and capacitance–frequency (*C–f*) curves were measured under dark condition using an Autolab PGSTAT-30 equipped with a frequency analyser module. The *J–V* measurements were performed first on the un-annealed noted as (as cast) and annealed device. For the annealed device, the heating process was carried out by putting the device on a hot plate (for 10 min) at different temperatures ranging from 40 to 130°C, and the *J–V* curves were measured for each annealing temperature. We note that the temperature of 130°C is reported to be as the optimum annealing temperature for the DPP(TBFu)$_2$ [17].

3. Results and discussion: Figs. 2*a* and *b* show the *J–V* characteristics for the ITO/DPP(TBFu)$_2$/Al device at different annealing temperatures from 40 to 130 °C. It is visible from this figure that the *J–V* characteristics are asymmetric with an exponential variation of the current upon forward bias. Indeed, the asymmetric variation of the *J–V* curves indicates Schottky like character [18, 19] of the ITO/DPP(TBFu)$_2$/Al device, and thus the formation of rectifying contact at the DPP(TBFu)$_2$/Al interface.

It is well known that the charge transport taking place at such metal/semiconductor contact is usually treated and analysed on the basis of thermionic, Poole–Frenkel emissions, ohmic, or space charge limited models [20]. The three former models are found to be inapplicable for our device in the selected voltage range as revealed by treating the data with their respective laws. By contrast, the *J–V* data showed an ambiguous agreement with the thermionic emission. In this case, the *J–V* relationship is expressed as follows [21]:

$$I = I_0\left[\exp\left(\frac{qV - IR_s}{\eta kT}\right) - 1\right] \quad (1)$$

Here, q is the elementary charge, V is the applied bias, k is the Boltzmann constant, R_s represents the series resistance, and I_0 stands for the saturation current which is given by the following equation [20]:

$$I_0 = A^* T^2\left[\exp\left(-\frac{q\Phi_B}{kT}\right)\right] \quad (2)$$

where A^* is the Richardson constant and Φ_B is the Schottky barrier height.

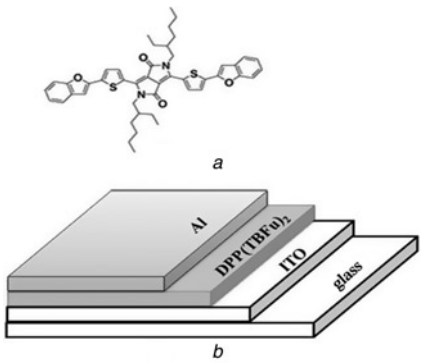

Fig. 1 *Molecular structure of DPP(TBFu)$_2$, and the corresponding sandwich arrangement*
a Chemical structure of DPP(TBFu)$_2$
b Sandwich arrangement representation of the studied device

However, curves illustrating the *J–V* characteristics do not tend to saturate to steady values in the higher voltage, indicating the absence of the series resistance effect in the explored voltage range. Therefore, it seems that the model taking into account the effect of the series resistance may not be valid in interpreting our *J–V* data. A model that does not take into account the series resistance was used. This model is described by the following expression:

$$I = I_0\left[\exp\left(\frac{qV}{\eta kT}\right) - 1\right] \quad (3)$$

By fitting of the *J–V* data with (3), we have estimated the diode parameters at the corresponding annealing temperatures such as the ideality factor (η), the barrier height (Φ_B) at the DPP/Al contact, the saturation current density (J_0), and the turn-on voltage (V_{th}) which corresponds to the applied forward bias just when the diode's current begins to increase from the current baseline of the *J–V* curve. The calculated parameters before and after annealing processes are stated in Table 1.

It is visible that most of the diode parameters remain almost unchanged upon annealing temperatures with the exception of the turn-on voltage (V_{th}). Remarkably, an increase of V_{th} (from an initial value of 1.6 V) starting from 70°C is noticed, and then remains constant after reaching a maximum value of 2.08 V at 100°C. This increase of V_{th} is probably caused by the following annealing effects: (i) at lower annealing temperatures (≤70°C), the presence of residual solvent might act as impurity centres that contribute to increase the free holes density that in turn influence the turn-on voltage. Indeed, it has been reported that defect centres in organic semiconductors might increase the doping

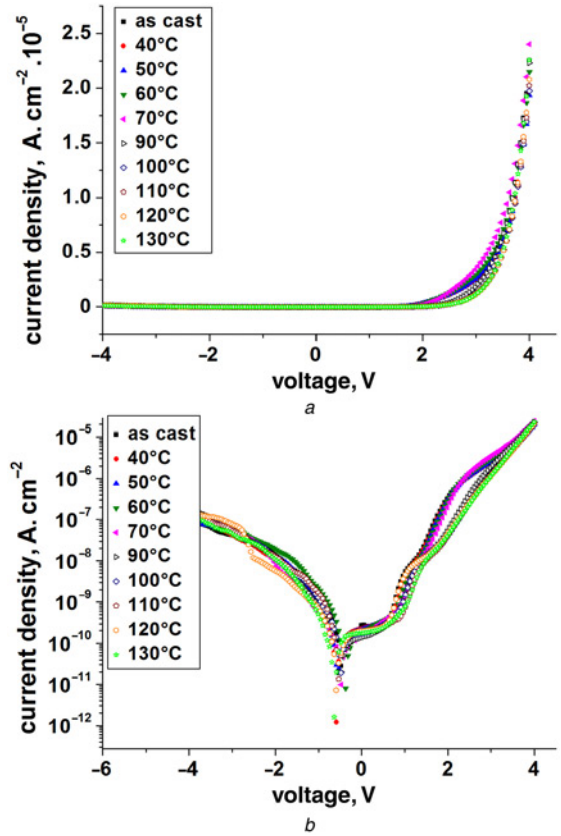

Fig. 2 *J–V characteristics for the ITO/DPP(TBFu)$_2$/Al device*
a Linear
b Semi-log plots of current density–voltage characteristics for different annealing temperatures

Table 1 Extracted diode parameters for different annealing temperatures

Annealing temperature, °C	V_{th}, V	η	ϕ_B, eV	J_0, A cm$^{-1} \times 10^{-7}$
as cast	1.60	1.98	0.91	1.02
40	1.60	1.99	0.91	1.08
50	1.60	1.98	0.90	1.06
60	1.60	1.98	0.91	1.28
70	1.76	1.98	0.92	1.25
90	1.97	1.99	0.92	1.37
100	2.08	1.99	0.91	1.22
110	2.08	1.99	0.91	1.09
120	2.08	1.98	0.91	1.12
130	2.08	1.98	0.91	1.17

density by generating more free carriers [22]; and (ii) at higher annealing temperatures (≥70°C), the solvent evaporation is expected to be more and more important leading to the improved DPP(TBFu)$_2$-crystallinity [23, 24], and hence a downward shift of the DPP(TBFu)$_2$ quasi-Fermi level is also expected to occur under thermal treatment. This reduction of defect states produces the quasi-Fermi level down shift yielding as a result higher V_{th} values.

As we have just discussed, our fabricated device showed that DPP(TBFu)$_2$ forms Schottky contact with Al and, on the other hand, an ohmic contact with ITO. Therefore, this aspect fulfils the criteria for accurate C–V measurement. Fig. 3 shows the normalised C–V curves for the non-and annealed device at 130°C from −0.6 to 3 V at a constant frequency of 1 kHz.

It is visible from this figure that the C–V curves exhibit a planar trend at reverse bias and even at low forward bias for the annealed device and then increase in excess of the geometrical capacitance ($C_g \simeq 31$ nF · cm^{-2}). This increase of C–V curves is attributed to the formation of a depletion region near the Al cathode. In addition, the C–V curves do not show the full depletion at −0.6 V of reverse bias for both cases. For clarification, it is clearly seen that the non-annealed device shows higher depletion zone than the annealed one indicating that the diode begins to be fully depleted. Furthermore, the dielectric constant of the studied DPP(TBFu)$_2$ ($\varepsilon_r \sim 1.81$) is estimated from the C_g by means of the relation which describes the variation of the C_g against the material thickness defined as [25]

$$C_g = \varepsilon_r \varepsilon_0 (A/d) \tag{4}$$

where A is the area of the diode, ε_r and ε_0 are the dielectric constant and the permittivity of vacuum, respectively, and d is the thickness of the DPP(TBFu)$_2$ film.

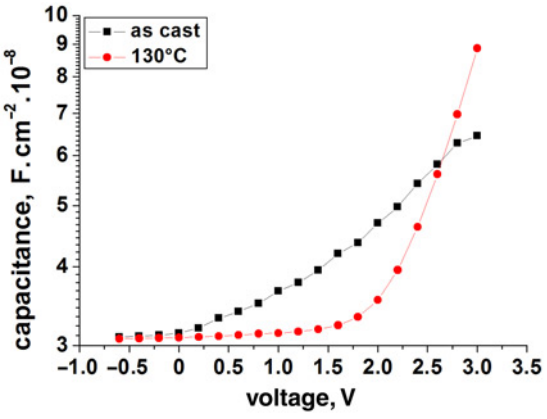

Fig. 3 *Normalised capacitance–voltage curve of ITO/DPP(TBFu)$_2$/Al device annealed at 130°C*

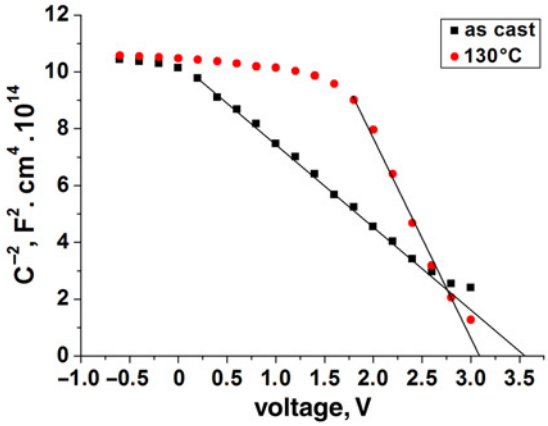

Fig. 4 *Mott–Schottky characteristic of DPP(TBFu)$_2$*

Considering C–V measurement that should help us in determining further device parameters, some developments are needed to be taken into consideration. In Fig. 4, we show typical Mott–Schottky curves corresponding to the non-annealed and annealed device at 130°C deduced from the well-known formula [26]

$$C^{-2} = \pm\left(\frac{2}{e\varepsilon_r\varepsilon_0 n}\right)\left(V - V_{fb-}\left(\frac{kT}{e}\right)\right) \tag{5}$$

where the positive sign is attributed to the n-type semiconductor nature, whereas the negative slope is instead for p-type behaviour. V_{fb} is the flat band potential which corresponds to the energy offset between the DPP(TBFu)$_2$ quasi-Fermi level and the Al work function, ε_r and ε_0 are the dielectric constant of the semiconductor and the permittivity of vacuum, respectively, kT is the thermal energy, and e represents the elementary charge.

Similarly to the C–V data, the C^{-2}–V plot does not show full depletion at −0.6 V of reverse voltages and exhibits a linear relationship at forward bias. The negative slope of the depletion zone lends an unambiguous evidence of p-type character of DPP(TBFu)$_2$ which takes its origin from carriers delocalisation through the material units. In addition, the concentration of defect states n and V_{fb} can be provided, respectively, from the extrapolated intersection with the potential axis and the slope of the straight line of the depletion regions; the estimated values of n are 9.57×10^{16} and 7.94×10^{16} cm^{-3}, and a flat band voltage shift from 3.09 to 3.54 V for the non-annealed and annealed devices, respectively. Interestingly, the total concentration of n confirms the highest defect density for the non-annealed device that corresponds to structural defects and to extrinsic impurities originated from the chemical solvent used during the processing. In contrast, for a device annealed at 130 °C, the defect density is lower than that observed for the non-annealed diode. Then, it appears that the difference in the defect concentration is mainly related to the presence of residual solvent that provide poorly crystalline DPP(TBFu)$_2$ film.

On the other hand, we were also able to obtain valuable information concerning the V_{fb} from the C^{-2}–V analysis. Importantly, annealing the device at 130°C results in a decrease of the V_{fb} from 3.09 to 3.54 V, suggesting the occurrence of a downward shift of the DPP(TBFu)$_2$ quasi-Fermi level. This is indeed in good accordance with the above prediction. It seems that it is possible to explain the increase of the V_{th} upon annealing processes by taking into account differences in n and V_{fb}. The V_{fb} position is linked to the effect of residual solvent that is regarded as a source of external impurities, contributing to the conductivity (p-doping). The quasi-Femi level undergoes a downward shift when the defect density within the DPP(TBFu)$_2$ bandgap is lower. Thus, the decrease of the charge carriers concentration

doi: 10.1049/mnl.2016.0318

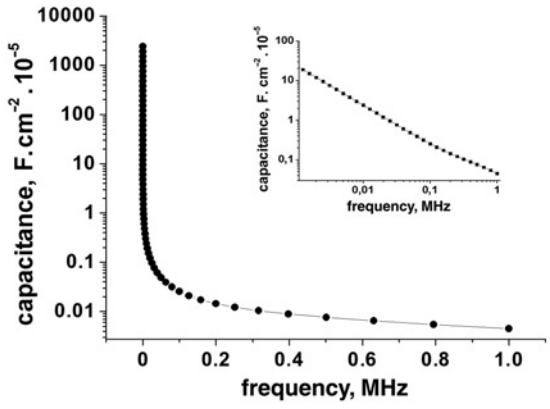

Fig. 5 *Normalised capacitance–frequency of ITO/DPP(TBFu)$_2$/Al device annealed at 130°C*

upon annealing appears to affect the conductivity and hence the turn on voltage of the studied diode.

Moreover, measurement of junction capacitance could yield valuable insights into the concentration of defect states within the gap of the active material. In the literature, there are two types of gap defects that can be defined from the *C–f* profile of such junction namely bulk and metal/semiconductor interface defects states. The first one is related to the appearance of a peak like response over the higher frequencies, while the lower frequencies peak comes from the states at the barrier contact. Typical *C–f* curve of the ITO/DPP(TBFu)$_2$/Al device (annealed at 130 °C) recorded at zero bias in the dark at room temperature is depicted in Fig. 5.

The *C–f* profile shows a non-proportionality of the capacitance values and the measuring frequencies. Initially, the capacitance is like sharply decreased over the low frequencies range until 80 kHz and then tends to stabilise. Actually, such behaviour is believed to be due to the presence of a distribution of localised states within the bulk material near the Al/DPP(TBFu)$_2$ interface [27]. In spite that the annealing at 130 °C improves the structural order, the distribution of localised states still exists within the active material which is an inherent property of organic semiconductors. Furthermore, a plateau corresponding to the greater frequencies (higher than 80 kHz) can be assigned to the geometrical capacitance C_g. The *C–f* profile in log–log scale depicted in Fig. 5 (inset) exhibits an increment of the capacitance toward low frequencies confirming the contribution of the gap defect states.

4. Conclusion: In conclusion, we have discussed the effect of annealing temperatures on the electrical properties of DPP (TBFu)$_2$-based Schottky diode. It was found that all the diode parameters remain almost unchanged upon annealing processes with the exception of the turn-on voltage. An increase of the turn-on voltage from 1.6 to 2.08 V was observed from 60 to 100°C, respectively. This fact has been attributed to the annealing induced crystallinity change which may influence on the free holes density. On the other hand, capacitance measurements revealed that the annealing process leads to a decrease in the density of defect states. This conclusion is supported by the downward shift of the quasi-Fermi level, which is reflected by the drop of the flat band potential.

5. Acknowledgments: This work was supported by the University of Sciences and Technology Houari Boumediene, Algeria.

6 References

[1] Singh J., Williams R.T.: 'Excitonic and photonic processes in materials' (Springer, Singapore, 2015)
[2] Montacada N.F., Pelado B., Viterisi A., *ET AL.*: 'High open circuit voltage in efficient thiophene-based small molecule solution processed organic solar cells', *Org. Electron.*, 2013, **14**, (11), pp. 2826–2832
[3] Xue S., Qiu X., Yao L., *ET AL.*: 'Fully solution-processed and multilayer blue organic light-emitting diodes based on efficient small molecule emissive layer and integrated interlayer optimization', *Org. Electron.*, 2015, **27**, pp. 35–40
[4] Tang W., Huang D., He C., *ET AL.*: 'Solution-processed small molecules based on indacenodithiophene for high performance thin-film transistors and organic solar cells', *Org. Electron.*, 2014, **15**, (6), pp. 1155–1165
[5] McCluskey F.P., Grzybowski R., Podlesak T.: 'High temperature electronics' (CRC Press, Boca Raton, 1997)
[6] Nafdey R.A., Kelkar D.S.: 'Schottky diode using $FeCl_3$-doped polyaniline', *Thin Solid Films*, 2005, **477**, (1–2), pp. 95–99
[7] Tsukamoto J., Ohigashi H., Matsumura K., *ET AL.*: 'Characteristics of Schottky barrier solar cells using polyacetylene, $(CH)_x$', *Synth. Method*, 1982, **4**, (3), pp. 177–186
[8] Tagmouti S., Outzourhit A., Oueriagli A., *ET AL.*: 'Electronic properties of poly(3-methylthiophene)', *Sol. Energy. Mater. Sol. Cells.*, 2002, **71**, (1), pp. 9–18
[9] Gupta R.K., Singh R.A.: 'Fabrication and characterization of Schottky diode based on composite organic semiconductors', *Compos. Sci. Technol.*, 2005, **65**, (3–4), pp. 677–681
[10] Shah M., Sayyad M.H., Karimov K.S.: 'Electrical characterization of the organic semiconductor Ag/CuPc/Au Schottky diode', *J. Semicond.*, 2011, **32**, (4), p. 044001
[11] Sharma A., Kumar P., Singh B., *ET AL.*: 'Capacitance-voltage characteristics of organic Schottky diode with and without deep traps', *Appl. Phys. Lett.*, 2011, **99**, (2), p. 023301
[12] Güllü O., Aydoğan S., Türüt A.: 'Fabrication and electrical characteristics of Schottky diode based on organic material', *Microelectron. Eng.*, 2008, **85**, (7), pp. 1647–1651
[13] Pahner P., Kleemann H., Burtone L., *ET AL.*: 'Pentacene Schottky diodes studied by impedance spectroscopy: doping properties and trap response', *Phys. Rev. B*, 2013, **88**, p. 195205
[14] Martinez-Landeros V.H., Gutierrez-Heredia G., Aguirre-Tostado F. S., *ET AL.*: 'Degradation of pentacene deposited on gold, aluminum and parylene surfaces: impact of pentacene thickness', *Thin Solid Films*, 2013, **531**, pp. 398–403
[15] Jeong S.G., Park H.Y., Lim M.H., *ET AL.*: 'Effect of post-fabrication thermal annealing on Fermi-level pinning phenomenon in metal-pentacene junctions', *Org. Electron.*, 2012, **13**, (9), pp. 1511–1515
[16] Lin Y., Zhan X.: 'Oligomer molecules for efficient organic photovoltaics', *Acc. Chem. Res.*, 2016, **49**, (2), pp. 175–183
[17] Kovalenko A., Honová J., Geerts Y., *ET AL.*: 'Effect of the side chains and anode material on thermal stability and performance of bulk-heterojunction solar cells using DPP(TBFu)$_2$ derivatives as donor materials', *Int. J. Photoenergy*, 2015, **2015**, p. 734917
[18] Nouchi R.: 'Extraction of the Schottky parameters in metal-semiconductor-metal diodes from a single current-voltage measurement', *J. Appl. Phys.*, 2014, **116**, (18), p. 184505
[19] Efron U.: 'Spatial light modulator technology: Materials, devices, and applications' (CRC Press, New York, 1994)
[20] Mansour M., Saidi M., Saidi-Amroun N.: 'Chemical synthesis and characterization of poly (o-methoxyaniline)', *Biointerface. Res. Appl. Chem.*, 2016, **6**, (2), pp. 1087–1092
[21] Sze S.M.: 'Physics of semiconductors devices' (Wiley, New York, 1969)
[22] Liang Z., Gregg B.A.: 'Compensating poly(3-hexylthiophene) reveals its doping density and its strong exciton quenching by free carriers', *Adv. Mater.*, 2012, **24**, (24), pp. 3258–3262
[23] Zhokhavets U., Erb T., Gobsch G., *ET AL.*: 'Relation between absorption and crystallinity of poly(3-hexylthiophene)/fullerene films for plastic solar cells', *Chem. Phys. Lett.*, 2006, **418**, (4–6), pp. 347–350
[24] Zhang Y., Dang X.D., Kim C., *ET AL.*: 'Effect of charge recombination on the fill factor of small molecule bulk heterojunction solar cells', *Adv. Energy Mater.*, 2011, **1**, (4), pp. 610–617
[25] Lungenschmied C., Bauer S., Schwödiauer R., *ET AL.*: 'Real-time in-situ observation of morphological changes in organic bulk-heterojunction solar cells by means of capacitance measurements', *J. Appl. Phys.*, 2011, **109**, (4), p. 044503
[26] Kirchartz T., Gong W., Hawks S.A., *ET AL.*: 'Sensitivity of the Mott–Schottky analysis in organic solar cells', *J. Phys. Chem. C.*, 2012, **116**, (14), pp. 7672–7680
[27] Viktorovitch P., Moddel G.: 'Interpretation of the conductance and capacitance frequency dependence of hydrogenated amorphous silicon Schottky barrier diodes', *J. Appl. Phys.*, 1980, **51**, (9), pp. 4847–4854